Optimizing Picket-Pulse-Shape Polar-Drive Implosion Designs

on the National Ignition Facility

Christopher Bosso

Penfield High School

Advisor: Radha Bahukutumbi

Laboratory for Laser Energetics

University of Rochester

Rochester, New York

December 2015

Abstract

In polar drive, laser beams configured for indirect drive on the National Ignition Facility (NIF) are displaced toward the target equator to achieve a more uniform direct-drive implosion. A NIF target consisting of multiple layers including CH (plastic), beryllium, and silicon-doped CH has been optimized for symmetry when irradiated with a triple-picket laser pulse shape. This pulse shape includes three pickets followed by a step and main pulse. The advantage of using a picket pulse shape over just a step and main pulse is the reduction of Rayleigh-Taylor instability, which contributes to the overall stability of the implosion. A combination of beam displacements and picket energy adjustments was used to create uniform shocks during each of the three pickets. The powers in the step and the main pulse were then adjusted, resulting in a significant increase in implosion uniformity. The laser beam profiles used in this design correspond to the so-called intermediate phase plates for direct drive on the NIF which were designed for CH capsules irradiated with two pickets. The optimization of this triple-picket pulse design with a multi-layer target suggests that the intermediate phase plates are sufficiently versatile to permit nearly uniform implosions with various ablators and laser pulse shapes.

I. Introduction

In direct-drive inertial confinement fusion (ICF) [1] laser beams directly irradiate a capsule consisting of a thin plastic shell with a solid cryogenic layer of deuterium-tritium. The outer region of the target then ablates, or expands, outwards while the center of the target is driven inwards in a rocket-like implosion resulting in high fuel temperatures and densities. Under these conditions, the deuterium and tritium nuclei fuse creating energetic neutrons and alpha particles. The neutrons escape the imploded capsule and can, in principle, be used to generate electricity by heating water. The alpha particles lose energy through collisions in the fuel and raise the temperature. This results in additional fusion reactions. Ignition is said to occur when more energy is released from the fusion reactions than the laser energy on-target .

Currently, there are two main techniques for irradiating the capsule. The first is direct drive (described above), where laser beams directly illuminate the target. The OMEGA Laser [2] at the University of Rochester is configured for direct drive with 60 nominally identical laser beams arranged symmetrically around the target and aimed at the center of the target. This results in a near-normal angle of incidence to the surface of the target of most of the laser energy. The second is indirect drive [3] where a target is placed inside a cylindrical container made of gold, known as a hohlraum. The hohlraum has laser entrance holes centered on the cylindrical axis through which the beams enter the hohlraum. X rays, emitted by the irradiation of the hohlraum, illuminate the target, thereby driving the implosion. The National Ignition Facility (NIF) [4] is configured for indirect drive with the beam ports at angles from 23° to 50° from the vertical axis.

While the OMEGA laser is useful in studying the physics of ICF, its maximum energy (30 kJ) is insufficient to achieve ignition. The NIF laser, with energy ~1.5 MJ, was designed for ignition. However, the beam configuration on the NIF was designed for indirect drive, which presents a significant challenge for direct drive. If the NIF beam configuration were used for direct drive with all beams aimed at the center of the target, it would result in an implosion whose uniformity was significantly compromised because the poles of the target would receive much more energy per unit area than the equator. A high degree of uniformity is essential for achieving the extreme levels of compression and temperature that are necessary to initiate ignition.

Improved uniformity can be obtained with polar drive [5], where beams are displaced from their original positions on the target surface. On the NIF, there are 192 beams which are grouped into 2x2 arrays called quads. These quads are arranged into four distinct rings in each hemisphere. If the beams are pointed at the center of the target, they strike the target with the pattern shown in Fig. 1a. In polar drive, these rings are displaced toward the equator or “repointed” to achieve better uniformity on the target. Ring 3 is also split into two separate rings, 3a and 3b, to further increase the uniformity of energy distribution over the surface of the target (Fig. 1b). Because the

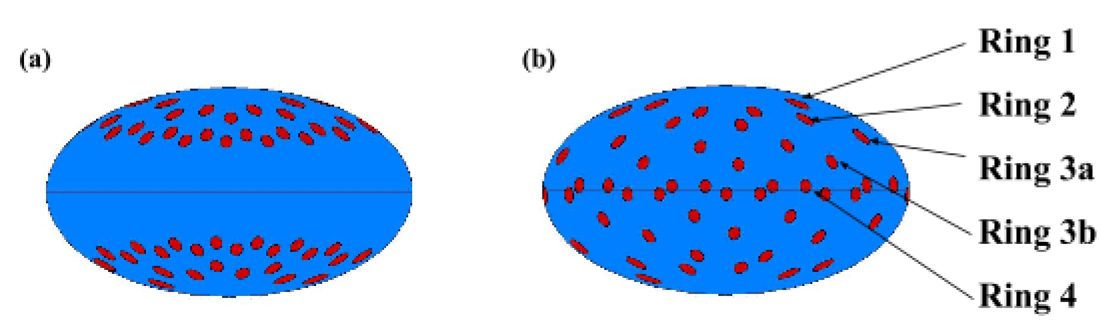

Figure 1: (a) NIF beam pointing configuration that would result from aiming all beams to the center of the target. Each red spot represents a quad. (b) Optimized polar drive beam pointings . Note that Ring 3 is split into two rings.

beams are shifted from their original normal angle of incidence, the repointed beams strike the surface of the target at more oblique angles of incidence. This results in the laser energy being deposited over a wider area of the target surface at more oblique angles, which equates to a reduction in drive.

Although the use of polar drive significantly improves the uniformity of the on-target beam arrangement, it also introduces various complications such as the need for different beam energies in each ring to compensate for the increasingly oblique angles of incidence as the beams are displaced further from their original positions. Additional improvements to the irradiation uniformity can be made through the optimization of the laser pulse shapes, beam energies, and the spatial cross-section of each laser beam (beam profiles).

In this paper, the optimization of a multi-layer room-temperature capsule is described. The beam profiles, the capsule parameters, and the total laser power as a function of time are given and the beam pointings and relative laser powers are adjusted to provide maximum uniformity. Beam profiles determine the intensity of the beam and are characterized by a high intensity center and then decreasing intensity towards the edges of the beam. These profiles are engineered using expensive optics known as phase plates. It is therefore important to ensure that the phase plates can be used to drive a variety of designs with a high degree of uniformity. The primary goal is to identify if the previously determined beam profiles for a plastic-only capsule [6] can be used to drive a multi-layer target near-spherically.

II. Target Design

The target considered in this paper (shown in Fig. 2b) is a spherical capsule with an outer radius of approximately 1295 μm and includes a 53 μm thick shell with multiple layers encasing compressed deuterium gas. The capsule contains layers of plastic (CH), beryllium, silicon, and a doped-CH layer (doped with 6% Si). The inner CH layer

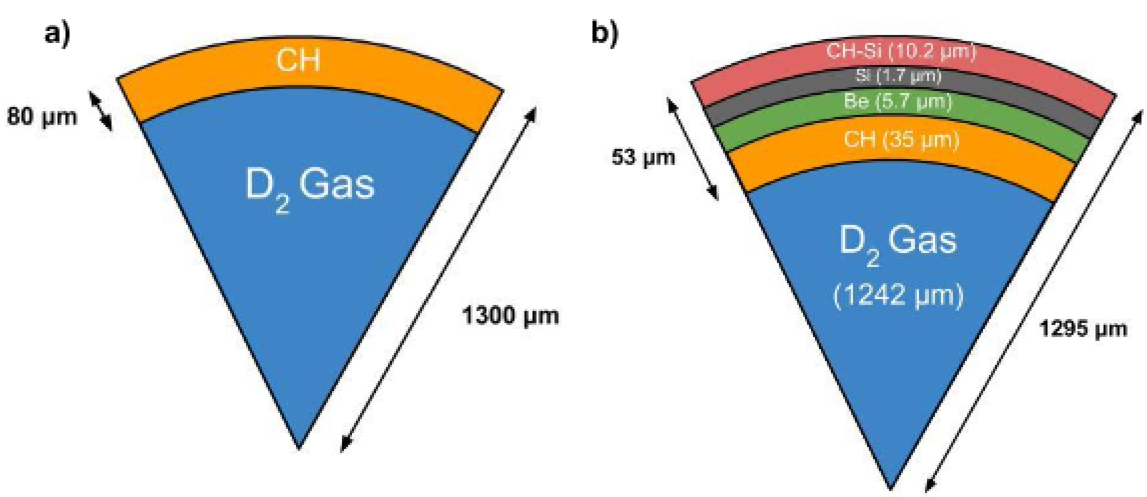

Figure 2: (a) Cross section of a 1300 μm CH-ablator target (b) Cross section of a multilayer, 1304 μm radius room-temperature target. The purpose of the extra layers is to increase the stability of the implosion.

serves as a surrogate for the cryogenic layer. A surrogate target can be imploded more easily on the NIF as it does not require the hardware necessary for cryogenic implosions. This target design can therefore be used to study the physics of the implosion without actually imploding cryogenic targets. In an ignition-relevant implosion experiment, the inner CH shell would be replaced with cryogenic deuterium-tritium ice.

The multilayer target is different from the typical CH ablator design (shown in Fig. 2a) used in many fusion experiments. Surrounding the innermost plastic shell is a 5.7 μm thick layer of beryllium. Material properties of Be make it a superior ablator to CH. This layer is then surrounded by a 1.7 μm thick layer of silicon and a 10.2 μm thick layer of silicon-doped plastic. The Si-doped layer has been shown to mitigate laser imprint (the imposition of the single beam nonuniformity on the target) [7] whereas the pure Si layer is expected to mitigate laser-plasma interactions (LPI) that can compromise the compression of the target [8]. The advantages of this multi-layered fusion target as opposed to the CH ablator design are a significant increase in the stability of the implosions, the increased energy coupled to the imploding shell, and mitigation of LPI instability. This design, therefore, can potentially compress more effectively than a target with only a CH ablator, therefore producing more neutrons.

Another crucial part of the target design is the laser beam pulse shape that describes the changes in single beam power over the course of the implosion. Laser pulse shapes can be adjusted independently for each ring of quads, making them a useful tool for tuning and optimizing polar drive implosions. The overall length of the laser pulse is determined by the energy available on the laser system. Up to 700 kJ is normally available to implode room-temperature targets on the NIF.

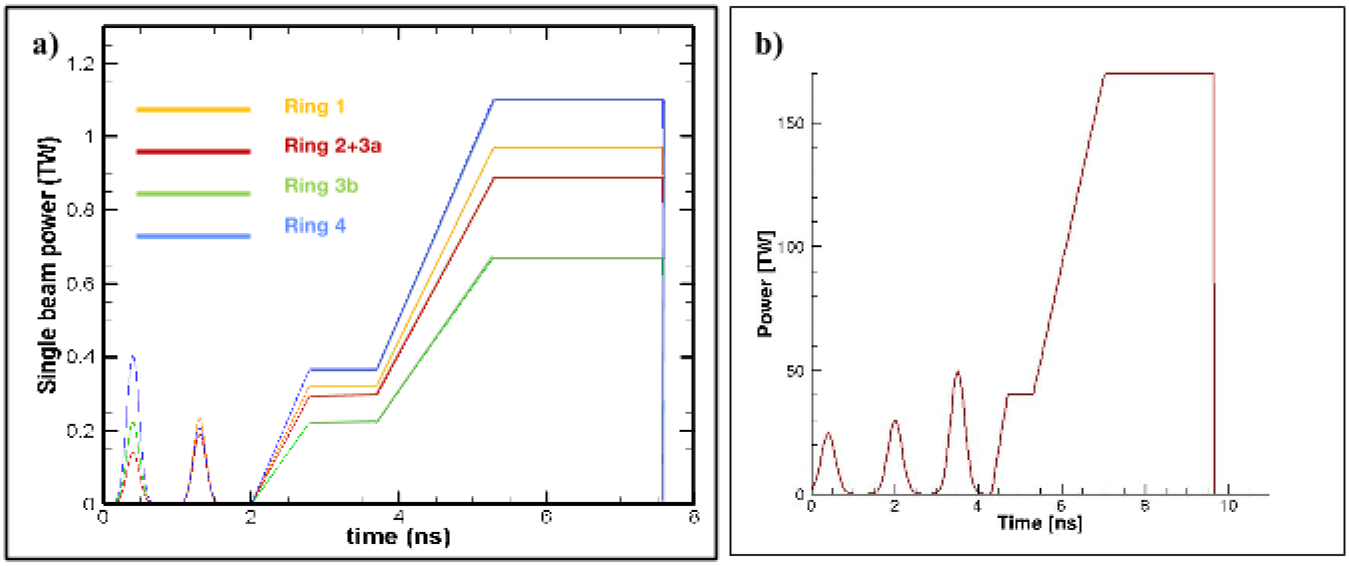

Figure 3. (a) The double-picket pulse shape for the CH-ablator design showing the beam power in terawatts for each ring. Note that Rings 2 and 3a have identical pulse shapes. (b) The base triple-picket pulse shape used in this work, with the power summed over all 192 beams.

Shown in Figure 3a are the laser pulse shapes for the CH-ablator implosion. Preceding the main pulse, there are two jumps or spikes in single-beam power known as "pickets." These picket pulses generate shocks that travel through the shell of the target and decrease Rayleigh-Taylor instability growth [9] of the target implosion. Following these two picket pulses is a brief jump in power known as a "foot," which also launches a shock into the shell. This is followed by the slow rise to the main pulse, which is meant to compress the target adiabatically, meaning that preheat of the target shell is minimized. This results in an effective compression of the target. A triple-picket pulse (Fig. 3b) before the main pulse is more effective than a double picket pulse to achieve higher compression. In a triple-picket pulse shape implosion, there are four shocks launched into the shell that precede the main pulse, one for each of the three picket pulses and then one for the foot pulse before the rise to the main pulse. The shocks move through the shell first, compressing it, and then break out of the shell and move into the internal D_2 gas. This transition between the layers during the implosion is called a "shock breakout". The beam pulse shape explored in this work is a triple-picket pulse in combination with a multi-layer target (Fig. 3b). Because there are differences in coronal absorption between the CH ablator target and the multi-layer target, the beam pointings and energies must be readjusted to achieve a uniform implosion using the pre-designed beam profiles.

III. Improving Uniformity

The hydrodynamics modeling code *DRACO* [10] was used to simulate implosions of a multi-layer target with a triple-picket pulse beam shape and identify an optimal set of parameters to maximize uniformity. A systematic approach was employed by first modifying the beam pointings to achieve better uniformity of the initial on-target intensity. Then, the laser-beam picket power ratios in each of the rings were adjusted to reduce nonuniformity at each of the shock breakouts created by the picket pulses before finally optimizing the foot and main pulse to achieve greater overall uniformity throughout the implosion.

It is necessary to keep the initial conditions of the implosion as uniform as possible because any nonuniformity which is introduced early on in the implosion will grow due to the converging shell. Therefore, by optimizing the picket pulse shock breakouts in the order in which they occur, uniformity can be maintained throughout the entire implosion.

	Original θ (CH Ablator)	Repointed θ (Multi-layer)
Ring 1	22.94	27.0
Ring 2	45.0	38.0
Ring 3a	45.0	56.0
Ring 3b	83.48	70.0
Ring 4	83.48	87.0

Table 1: Original and repointed angles for the rings. Rings were displaced only in their polar angle. Beams were equally spaced in the azimuthal direction within each ring.

The beam pointings from the CH ablator model shown in Table 1 were used as a starting point for this optimization and adjusted to account for the multi-layer target and triple-picket pulse shape. These beam pointings define the positions of the rings in the northern hemisphere only. Beam displacements are identical in the southern hemisphere. A polar angle of 0° corresponds to the pole and 90° corresponds to the equator. Since the northern and southern hemispheres are symmetric, only the northern hemisphere is simulated in this work. The same improved beam pointings are shown in Fig. 1b.

The initial normalized on-target intensity as a function of polar angle, shown in Figure 4, provided insight into the improved beam pointings that reduce nonuniformity. Regardless of the target type, a higher on-target intensity at the equator compared to the pole is required to compensate for the reduced energy absorption from the oblique angles of incidence of the repointed beams. However, during early runs the intensity at

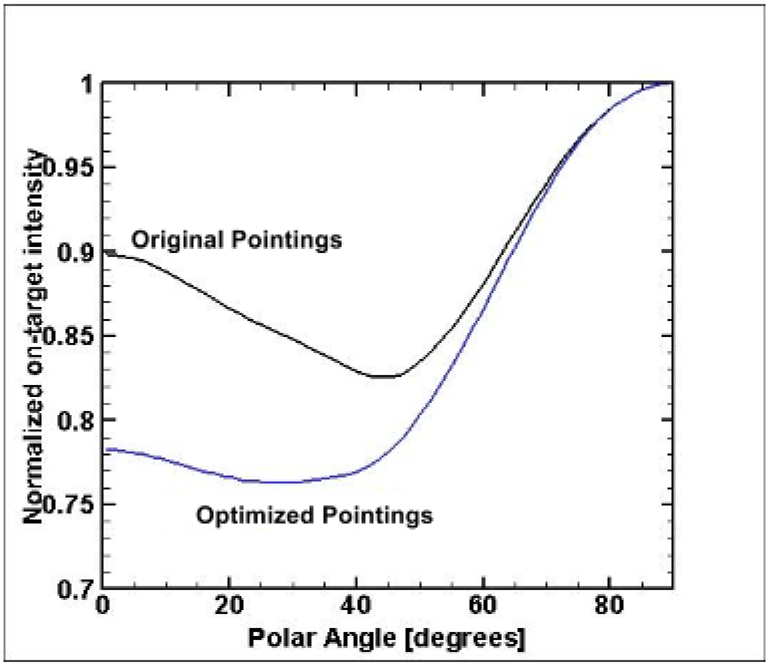

Figure 4. Initial normalized on-target intensity at 0 ns for an implosion with original beam pointings and the on-target intensity at 0 ns for an implosion with optimized pointings.

the pole was larger than required, leading to nonuniformities (corresponding to "original pointing" in the Fig. 4). This was identified by the nonuniform first shock in the shell. Therefore, a set of beam pointings were identified where the rings were repointed more toward the equator. This reduced the intensity near the pole, improved the initial on-target uniformity (corresponding to "optimized pointing" in Fig. 4), and resulted in a more uniform first shock.

In Figure 5, a density contour plot is shown at the time of the first picket pulse shock breakout for the original pointings and beam power ratios using a triple picket pulse shape (Fig. 5a), and for the improved pointing and beam power ratios (Fig. 5b).

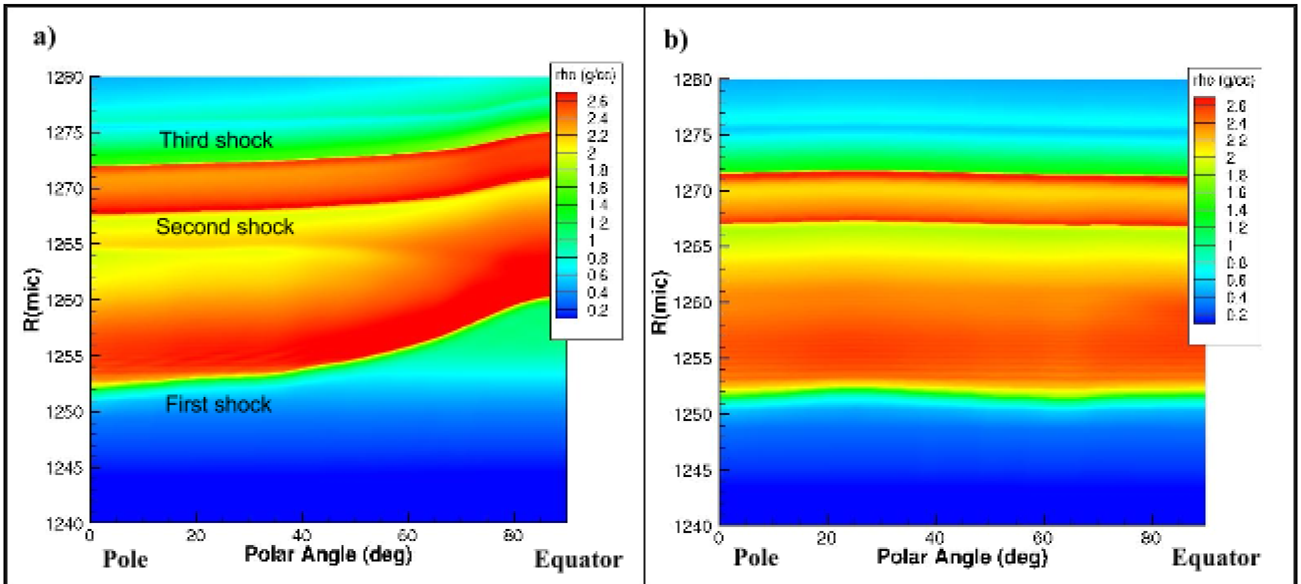

Figure 5. (a) Density contour plot at first picket pulse shock breakout for a multi-layer target with original pointings and ring power ratios. (b) Density countour plot at first picket pulse shock breakout for a multi-layer target with optimized pointings and ring power ratios.

There is a noticeable lack in drive at the equator compared to the pole in Fig. 5a due to differences in coronal absorption between the multi-layer target and the CH ablator target for which the original pointings were designed. A more uniform shock breakout of the multi-layer target was obtained with optimized pointings and beam power ratios. To achieve this greater uniformity, systematic changes were made to the beam power ratios for each ring at different stages of the implosion. For the first shock breakout, beam power ratios were modified between 0 ns and 1.5 ns. The same process was used to optimize the shock from the second picket.

Of the three picket pulses, the third was shown to have the greatest impact on the overall uniformity of the implosion. The third picket pulse shock breakout (shown in Fig. 6) was also optimized for uniformity using incremental modifications to beam power

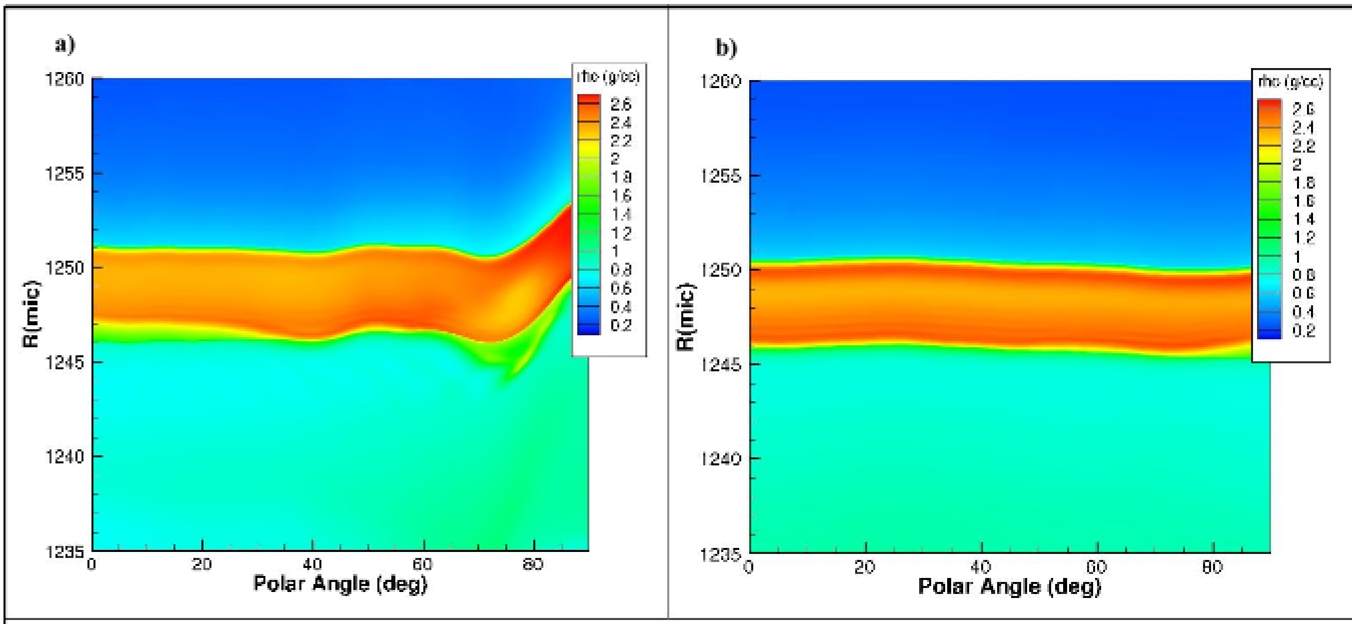

Figure 6. (a) Density contours of multi-layer target with original pointings and beam power ratios at the time of third shock breakout. (b) Density contours of multi-layer target with optimized pointings and beam power ratios at the time of third shock breakout.

ratios until a uniform shock breakout was achieved. As shown in Figure 6, the uniformity during the third shock breakout can be greatly improved with changes to beam pointings and power ratios. This systematic method of optimization was then employed to optimize the shock created by the foot pulse in order to achieve a high degree of uniformity throughout the entire implosion leading up to the main pulse. The final pulse shape for the implosion is shown in Figure 7 with all of the optimized beam power ratios. The pulse shapes for rings 3a

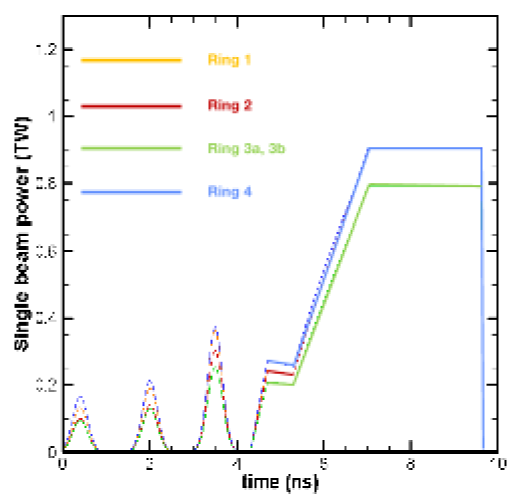

Figure 7. Laser pulse shapes for all five rings for the optimized multi-layer target design with a triple-picket pulse. During the main pulse, the red curve overlaps with the blue and the yellow curve overlaps with the green.

and 3b must be the same because both originate from one ring, although slight differences in the energy ratio between the two rings are tolerable. Here, the ratio is kept to 1. Optimizing past shock breakout was accomplished by adjusting the power of each ring during the main pulse to maintain the uniformity of the imploding shell. The late-time results of the implosion using the optimized laser pulse shape and beam pointings are shown in Fig. 8b, along with a late-time implosion of a multi-layer target with the original pointings and beam energies. Here it is easy to see the improvement on the late-time uniformity of the implosion at peak compression.

Hot spot distortion is defined as the ratio of the root-mean-square deviation of the

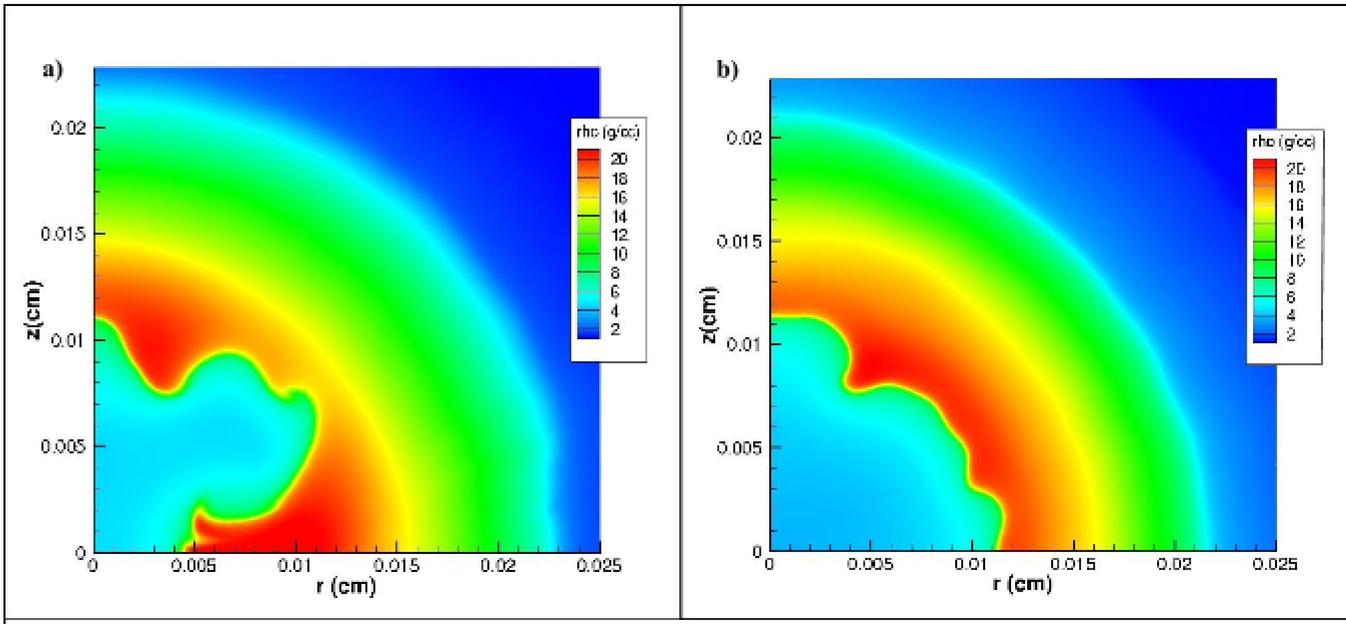

Figure 8: Density contours at a convergence ratio of 11 (10.1 ns) for (a) an implosion of a multi-layer target with the original beam pointings and power ratios and (b) an implosion of the same target using optimized beam pointings and power ratios.

inner fuel-shell interface from the average radius of the interface and can be used as a quantitative measure of nonuniformity of the compressed core. In Fig. 8a, the hot spot distortion is calculated to be 8.5%, while the hot spot distortion of Fig. 8b is 3.9%. This shows that hot spot distortion can be reduced by more than half with changes to just beam pointings and beam energies.

IV. Conclusion

Simulations were carried out using the 2D hydrodynamics code DRACO to optimize the uniformity of a multi-layer target driven by a triple-picket pulse shape using pre-designed beam profiles. A combination of picket energy adjustments and beam repointings were used to create uniform shocks during each of the three pickets and then further adjustments were made to the foot and main pulses to achieve excellent uniformity at peak compression in the implosion. These results suggest that the pre-designed beam profiles are versatile and permit nearly uniform implosions when targets and pulse shapes are varied. The versatility of the beam profiles is of great value because the optics that are used to obtain these profiles on laser facilities are expensive to manufacture and difficult to change once they are in place. The ability to implode varying designs with fixed hardware significantly improves the ability to explore implosion physics.

V. Acknowledgements

I would like to thank those who helped me in the completion of my project and this report and everyone who made my time at LLE such an incredible experience. First, I'd like to thank Dr. Stephen Craxton for giving me the opportunity to take part in this amazing program and for all the work he has done to give other high school students this experience each year. Second, I'd like to thank all the participants in this year's high school program for making our work environment so fulfilling and enjoyable and helping me whenever I needed assistance. Third, I'd like to thank Felix Weilacher for all the knowledge and expertise he's shared with me and his continual motivation and support of me throughout my time at LLE. Finally, I'd like to give special thanks to my advisor, Dr. Radha P. Bahukutumbi, for all the countless hours of work she put into designing my project and for her patience and understanding as she guided me through the obstacles and difficulties to reach a successful end to my project.

References

1. J. Nuckolls, L. Wood, A. Thiessen, and G. Zimmerman, Nature **239**, 139 (1972).
2. T. R. Boehly, D. L. Brown, R. S. Craxton, R. L. Keck, J. P. Knauer, J. H. Kelly, T. J. Kessler, S. A. Kumpan, S. J. Loucks, S. A. Letzring, F. J. Marshall, R. L. McCrory, S. F. B. Morse, W. Seka, J. M. Soures, and C. P. Verdon, Opt. Commun. **133**, 495 (1997).
3. J. D. Lindl, "*Inertial confinement fusion: the quest for ignition and energy gain using indirect drive",* American Institute Of Physics, 1998.
4. C. A. Haynam, P. J. Wegner, J. M. Auerbach, M. W. Bowers, S. N. Dixit, G. V. Erbert, G. M. Heestand, M. A. Henesian, M. R. Hermann, K. S. Jancaitis, K. R. Manes, C. D. Marshall, N. C. Mehta, J. Menapace, E. Moses, J. R. Murray, M. C. Nostrand, C. D. Orth, R. Patterson, R. A. Sacks, M. J. Shaw, M. Spaeth, S. B. Sutton, W. H. Williams, C. C. Widmayer, R. K. White, S. T. Yang, and B. M. Van Wonterghem, Appl. Opt. **46**, 3276 (2007).

5. S. Skupsky, J. A. Marozas, R. S. Craxton, R. Betti, T. J. B. Collins, J. A. Delettrez, V. N. Goncharov, P. W. McKenty, P. B. Radha, T. R. Boehly, J. P. Knauer, F. J. Marshall, D. R. Harding, J. D. Kilkenny, D. D. Meyerhofer, T. C. Sangster, and R. L. McCrory, Phys. Plasmas **11**, 2763 (2004).
6. D. Cao, J. Marozas, T. Collins, P. B. Radha, and P. W. McKenty, "*An Intermediate Far Field Design for Polar Direct Drive at the National Ignition Facility*", presented at the 57th Annual Meeting of the Division of Plasma Physics, Savannah, GA, 2015.
7. Fiksel, G., S. X. Hu, V. A. Goncharov, D. D. Meyerhofer, T. C. Sangster, V. A. Smalyuk, B. Yaakobi, M. J. Bonino, and R. Jungquist, Phys. Plasmas **19**, 062704 (2012).
8. J. Myatt, H. X. Vu, D. F. DuBois, D. A. Russell, J. Zhang, R. W. Short, and A. V. Maximov, Phys. Plasmas **20**, 052705 (2013).
9. Lord Rayleigh, Proc. London Math Soc. **XIV**, 170 (1883); G. Taylor, Proc. R. Soc. London Ser. A **201**, 192 (1950).
10. P. B. Radha, V. N. Goncharov, T. J. B. Collins, J. A. Delettrez, Y. Elbaz, V. Yu. Glebov, R. L. Keck, D. E. Keller, J. P. Knauer, J. A. Marozas, F. J. Marshall, P. W. McKenty, D. D. Meyerhofer, S. P. Regan, T. C. Sangster, D. Shvarts, S. Skupsky, Y. Srebro, R. P. J. Town, and C. Stoeckl, Phys. Plasmas **12**, 032702 (2005).